

Loss of p53 Induces Tumorigenesis in p21-Deficient Mesenchymal Stem Cells^{1,2}

Rene Rodriguez*, Ruth Rubio*, Manuel Masip*, Purificación Catalina*, Ana Nieto*, Teresa de la Cueva*, Mar Arriero†, Nuria San Martín†, Ernesto de la Cueva‡, Dimitrios Balomenos§, Pablo Menendez* and Javier García-Castro*

*Andalusian Stem Cell Bank (BACM)/University of Granada, 18100 Granada, Spain; †Hospital Infantil Niño Jesús, 28009 Madrid, Spain; ‡Cancer Research UK Cambridge Research Institute, Cambridge CB2 0RE, UK; §Centro Nacional de Biotecnología/Consejo Superior de Investigaciones Científicas (CSIC), 28049 Madrid, Spain

Abstract

There is growing evidence about the role of mesenchymal stem cells (MSCs) as cancer stem cells in many sarcomas. Nevertheless, little is still known about the cellular and molecular mechanisms underlying MSCs transformation. We aimed at investigating the role of p53 and p21, two important regulators of the cell cycle progression and apoptosis normally involved in protection against tumorigenesis. Mesenchymal stem cells from *wild-type*, *p21*^{-/-}*p53*^{+/+}, and *p21*^{-/-}*p53*^{+/-} mice were cultured *in vitro* and analyzed for the appearance of tumoral transformation properties after low, medium, and high number of passages both *in vitro* and *in vivo*. *Wild-type* or *p21*^{-/-}*p53*^{+/+} MSCs did not show any sign of tumoral transformation. Indeed, after short-term *in vitro* culture, *wild-type* MSCs became senescent, and *p21*^{-/-}*p53*^{+/+} MSCs showed an elevated spontaneous apoptosis rate. Conversely, MSCs carrying a mutation in one allele of the *p53* gene (*p21*^{-/-}*p53*^{+/-} MSCs) completely lost p53 expression after *in vitro* long-term culture. Loss of p53 was accompanied by a significant increase in the growth rate, gain of karyotypic instability, loss of p16 expression, and lack of senescence response. Finally, these cells were able to form fibrosarcomas partially differentiated into different mesenchymal lineages when injected in immunodeficient mice both after subcutaneous and intra-femoral injection. These findings show that MSCs are very sensitive to mutations in genes involved in cell cycle control and that these deficiencies can be at the origin of some mesodermic tumors.

Neoplasia (2009) 11, 397–407

Abbreviations: CDK, cyclin-dependent kinase; CIN, chromosome instability; CPT, camptothecin; HSC, hematopoietic stem cell; MEF, mouse embryonic fibroblast; MSC, mesenchymal stem cell

Address all correspondence to: Javier García-Castro, PhD, Andalusian Stem Cell Bank (BACM), Centro de Investigación Biomédica, University of Granada, Parque Tecnológico de la Salud, Avda. del Conocimiento s/n, 18100 Granada, Spain.

E-mail: javier.garcia.castro.exts@juntadeandalucia.es, Web site: www.juntadeandalucia.es/bancoandaluzdecelulasmadre

¹This work was funded by the Consejería de Salud de la Junta de Andalucía (grants 0108/2007 to R.R., 0028/2006 and 0029/2006 to P.M., and 0027/2006 to J.G.-C.), Consejería de Educación de la Comunidad Autónoma de Madrid (S-BIO-0204-2006; MESENCAM), The International Jose Carreras Foundation against the Leukemia to PM (EDThomas-05), and The Spanish Ministry of Health to P.M. (FIS PI070026) and to J.G.-C. (FIS PI052217).

²This article refers to supplementary materials, which are designated by Figures W1 to W3 and are available online at www.neoplasia.com.

Received 17 December 2008; Revised 19 January 2009; Accepted 21 January 2009

Introduction

The cyclin-dependent kinase (CDK) inhibitor p21^{Cip1/Waf1} (hereafter referred to as p21) is regulated by both p53-dependent and -independent mechanisms on cellular stress, and the induction of p21 may cause cell cycle arrest [1,2]. In addition to the loss of cell cycle checkpoints, p21 deficiency commonly results in the lack of both replicative and DNA damage-induced senescence [3,4] and the increase of apoptosis after several stresses [5,6].

Unlike *p53-deficient* (*p53*^{-/-}) mice, *p21-deficient* (*p21*^{-/-}) mice are resistant to early onset of tumorigenesis [7], although they develop spontaneous tumors at an average age of 16 months. Remarkably, half of these tumors long-term developed by *p21*^{-/-} mice display a mesoderm origin (i.e., histiocytic sarcomas) [8]. Moreover, p21 deficiency was shown to facilitate the susceptibility to sarcomas in *p53*^{+/-} and *p53*^{-/-} mice [9]. Mouse embryonic fibroblasts (MEFs) derived from *p21*^{-/-} mice show a greater capacity to grow at late passages compared with wild-type MEFs [7]. Similarly, p21 knockdown in human fibroblasts allows cells to bypass senescence, although eventually, they enter a nonproliferative crisis state [3,10].

The consequences of p21 deficiency in adult stem cells have been studied in hematopoietic stem cells (HSCs), neural stem cells, and endothelial progenitor cells. In these cell types, p21 seems to control their development and proliferation. *p21*^{-/-} mice have more HSCs than normal mice and fewer stem cells are in a quiescent state [11]. Similar to HSCs, p21 contributes to the relative quiescence of adult neural stem cells and the loss of p21 lead to the exhaustion of their self-renewal capacity [12]. Endothelial progenitor cells number and their clonal expansion capacity are also elevated in *p21*^{-/-} mice compared with wild-type counterparts [13].

Studies in mesenchymal stem cells (MSCs) show that the overexpression of p21 protect them from programmed cell death induced by low-density culture [14] and that there was an age-dependent decrease in the proliferation of MSCs associated with an up-regulation of p21 [15]. In addition, p53, the better known activator of p21, has also been reported to be mutated in a model of spontaneously transformed MSCs, which recapitulated the naturally occurring fibrosarcomas observed in aged mice [16]. However, there is no information about the effects of p21 deficiency in MSCs.

Previous reports suggest that MSCs could behave as cancer stem cells of certain sarcomas [17–21] and that their *in vitro* transformation would also generate both sarcomas [16,22–24] and carcinomas [25,26]. Little is still known, however, about the cellular and molecular mechanisms underlying MSCs transformation. The process of MSCs transformation has been associated to the accumulation of chromosome instability (CIN) [22–24] and high resistance to apoptosis [27], suggesting the relevance of an accurate cell cycle control in MSCs. In fact, alterations in cell cycle regulators such as p16^{INK4A}, p53, and CDK-1, CDK-2, and CDK-6 [21,23,28] have been detected in transformed MSCs.

On the basis of the relation between p21 deficiency and sarcomagenesis and in the ability of transformed MSCs to generate sarcomas, we aimed to study the role of p21 and p53 during *in vitro* culture of murine MSCs (mMSCs). We have derived and grown MSCs from *p21*^{-/-} and *p21*^{-/-}*p53*^{+/-} mice. We found that *p21*^{-/-} MSCs grow with similar characteristics to that of wild-type MSCs, except for a greater apoptotic rate, and that these cells were not tumorigenic. Strikingly, on the introduction of a mutation in one allele of *p53* gene generating *p21*^{-/-}*p53*^{+/-} MSCs, we observed a complete loss of p53 function after continuous *in vitro* culture associated with a

malignant phenotype as shown by the ability of these cells to form sarcomas in immunodeficient mice.

Materials and Methods

Obtaining and In Vitro Culture of Mouse MSCs

p21^{-/-} and *p21*^{-/-}*p53*^{+/-} mice on a C57BL/6J background have been previously described and characterized [9,29]. Mesenchymal stem cells were derived from adipose tissue. The tissue was cut into small pieces and disaggregated for 2 hours, with the digestion medium consisting of Dulbecco's modified Eagle's medium (Gibco, Carlsbad, CA) with 1 mg/ml collagenase A (Roche, Basel, Switzerland). The sample was centrifuged, filtered through 40- μ m nylon filter (Becton Dickinson, Franklin Lakes, NJ), seeded at a density of 1.6×10^5 cells/cm² in flasks with MesenCult for mouse cells medium and MSC supplements (Stem Cell Technologies, Vancouver, Canada), and incubated at 37°C in a 5% humidified CO₂ atmosphere. After 24 hours, nonadherent cells were discarded, and fresh medium was added. When cell culture achieved more than 90% of density, adherent cells were trypsinized (0.25% trypsin; Sigma, St. Louis, MO), washed, and replated at a concentration of 4×10^3 cells/cm².

Flow Cytometry Analysis of MSCs

The immunophenotype of cultured MSCs was analyzed by flow cytometry. Cells were trypsinized, washed, and suspended in PBS with 1% bovine serum albumin (Sigma). A total of 2×10^5 cells were incubated in the dark for 30 minutes with fluorochrome-conjugated monoclonal antibodies (Sca-1, CD11b, CD34, CD45, CD44, and CD29; BD Biosciences, San Jose, CA), washed, and analyzed in a FACSCanto II cytometer (BD Biosciences).

Differentiation Studies of MSCs

Mesenchymal stem cells were plated at 5×10^3 cells/cm² in MesenCult medium and were allowed to adhere for 24 hours. Culture medium was then replaced with specific differentiation inductive media. For adipogenic differentiation, cells were cultured in Adipogenic MSCs Differentiation BulletKit (Lonza, Basel, Switzerland) for 2 weeks. Differentiated cell cultures were stained with Oil Red O (Amresco, Solon, OH). For osteogenic differentiation, cells were cultured in Osteogenic MSCs Differentiation BulletKit (Lonza) for 2 weeks. Differentiated cell cultures were stained with Alizarin Red S (Sigma).

In Vitro Cell Growth Analysis

Cell cultures were checked daily for changes in growth rates and morphology. Growth curves were performed by assessing the cell number in triplicate MSC cultures for 8 days. For colony-forming assays, cells were plated in triplicate at low density (2000 cells/100-mm dish). Cells were allowed to grow for 10 to 15 days before staining them with 0.5% crystal violet (Sigma)/25% methanol. Only colonies of >50 cells were scored.

Karyotypic Analysis

Cells were cultured in medium supplemented with 0.1 mg/ml colcemid (Sigma) for 3 to 4 hours, washed with PBS, and trypsinized. The subsequent pellet was carefully resuspended in hypotonic solution of KCl (0.075 M), incubated for 20 minutes at 37°C, spun down, and fixed in Carnoy's solution (methanol/acetic acid ratio, 3:1). The fixing procedure was repeated three times, and the pellet was finally resuspended in 1 ml of fixative. Cells were then dropped

on glass slides, and the chromosomes were visualized by using modified Wright's staining. Metaphases were analyzed using conventional microscope (Leica DM 5500B, Solms, Germany), and the karyotypes were prepared using IKAROS software (Metasystems, North Royalton, OH). Fifty metaphases were analyzed for each culture.

Cell Cycle Analysis

Cell cycle analysis was carried out by flow cytometry after propidium iodide staining of 70% ethanol-fixed cells as previously described [6].

Detection of Apoptosis

Apoptotic cells were assessed by flow cytometry using PE-Annexin V according to the manufacturer's instructions (BD Biosciences).

Senescence-Associated β -Galactosidase Staining

After the indicated treatments, cells were fixed and incubated overnight with X-gal solution (pH 6.0) as previously described [10].

In Vivo Tumorigenesis Assay

Nonobese diabetic/severe combined immunodeficient NOD.Cg-Prkdc^{scid} IL2rg^{tm1Wjl/SzJ} (NOD/SCID-IL2R^{-/-}) mice were obtained from The Jackson Laboratory (Bar Harbor, ME). All mice were housed under specific pathogen-free conditions, fed *ad libitum* according to Animal Facilities guidelines, and used at 8 to 12 weeks of age. All protocols involving mice were approved by the Institutional Animal Care and Use Committee. Female NOD/SCID-IL2R^{-/-} mice were infused subcutaneously with 3×10^6 cells. According to the UKCCCR guidelines for the welfare of animals in experimental neoplasia, animals were killed when their tumors reached approximately a diameter of 10 mm or 5 months after inoculation. Tumors and organs extracted for further analyses. In some experiments, a fraction of tumors was incubated in culture medium containing 1 mg/ml collagenase A for 3 hours. Then, disaggregated samples were centrifuged, filtered through 40- μ m nylon filter, and seeded in culture as described above to reestablish *ex vivo* culture of tumor cells.

Histologic Analysis

Tumor samples were fixed in 4% buffered formalin, embedded in paraffin wax, cut into 4 μ m sections, and stained with hematoxylin and eosin. The histologic diagnosis was performed following the criteria of the World Health Organization described by Ernst et al. [30] taking in account the infiltrative growth, cellular pleomorphism, and cellular malignancy. Immunohistochemical staining was carried out using the ABC Vectastain Elite Kit (Vector Laboratories, Burlingame, CA) according to manufacturer's instructions and counterstained with hematoxylin. After a previous unmasking antigen with heat and blocking unspecific protein with MOM kit (Vector Laboratories), the primary antibody antihuman β -tubulin III (Chemicon, Billerica, MA) was incubated at a dilution 1:100 for 1 hour at room temperature. Immunoreactivity was observed with 3-3' diaminobenzidine tetrahydrochloride (Vector Laboratories).

Western Blot Analysis

Whole-cell extracts were prepared after treatment with or without 0.5 μ M camptothecin (CPT; Sigma) for 24 hours as described previously [31], resolved on 10% SDS-PAGE gels, and blotted onto nitrocellulose (BioRad, Hercules, CA). Proteins were detected with the enhanced chemiluminescence detection system (Amersham,

Buckinghamshire, England) using anti-p21 (sc-6246), anti-p53 (sc-6243), anti-p16 (sc-74401), and anti-c-myc (sc-41) from Santa Cruz Biotechnology, Santa Cruz, CA; anti-phospho-p53 (Ser15) (PC386) and anti-p19 (PC435) from Calbiochem, Darmstadt, Germany; or anti- β -actin (A1978) from Sigma.

Results

Characterization of p21^{-/-}p53^{+/+} and p21^{-/-}p53^{+/-} Mouse MSCs

Mesenchymal stem cells from *wild-type*, p21^{-/-}p53^{+/+}, and p21^{-/-}p53^{+/-} mice were maintained in culture for short-term (ST; passages 3-15), medium term (MT; passages 16-35) or long-term (LT; passages 36-60) periods. During ST *in vitro* culture, cells from all genotypes showed a typical fibroblast-like morphology (Figure 1A). However, after continuous culture, p21^{-/-}p53^{+/-} (MT and LT) MSCs changed from an elongated spindle shape to a small, compact morphology (Figures 1A and 2A). All these cell types showed their capacity to differentiate to adipocytes and osteocytes after specific stimulation as usual in MSCs (Figure 1A). Nevertheless, the p21^{-/-}p53^{+/-} (LT) MSCs showed poorer differentiation to the adipogenic lineage. After ST culture, all MSCs expressed the cell surface antigens Sca-1, CD44, and CD29 and lacked expression of the hematopoietic markers CD45, CD14, and CD11b, therefore displaying a common mouse-MSC phenotype [32,33] (Figure 1B). Intriguingly, after LT culture, p21^{-/-}p53^{+/-} MSCs had almost completely lost the expression of Sca-1, although the rest of the markers remain in a similar level of expression. Taken together, the changes observed in p21^{-/-}p53^{+/-} MSCs after long-term culture suggest a different *in vitro* homeostasis behavior.

In Vitro Immortalization of p21^{-/-}p53^{+/-} MSCs After Extensive Cell Culture

Ongoing experimental evidence suggests that normal MSCs, like most of primary cell cultures, enter senescence on several passages *in vitro* [34]. Here, after 10 to 15 passages, *wild-type* MSCs showed a pronounced increase in size with prominent and enlarged nuclei characteristic of senescent cells. In fact, the entire cell population stained for senescence-associated β -galactosidase activity (SA- β -gal; Figure 2A). After identical number of passages, p21^{-/-}p53^{+/+} MSCs showed a significantly lower level of senescence cells, although in these cultures, a high proportion of smaller, rounded, and partially detached apoptotic cells were detected (Figure 2A). Almost half of the p21^{-/-}p53^{+/+} MSCs undergoes spontaneous apoptotic response as quantified by Annexin V binding (Figure 2B). As a consequence of these antiproliferative effects (senescence and/or apoptosis), cultures of *wild-type* and p21^{-/-}p53^{+/+} MSCs did not progress any further. Conversely, p21^{-/-}p53^{+/-} MSCs did not undergo either senescence or apoptosis. Opposite to these effects, after 17 to 22 passages, a colony showing a small, rounded morphology arose in these cultures (Figure 2A). This cell population showed a growth rate much higher than the normal spindle-shaped cells and completely took over the entire culture after a few passages. As a consequence, p21^{-/-}p53^{+/-} (MT) MSCs displayed an immortalized/transformed phenotype that includes the loss of contact inhibition, a growth rate much higher than *wild-type*, p21^{-/-}p53^{+/+} or p21^{-/-}p53^{+/-} (ST) MSCs (Figure 2C) as a result of a higher mitotic index (data not shown), and the gain of clonogenic capacity (Figure 2D).

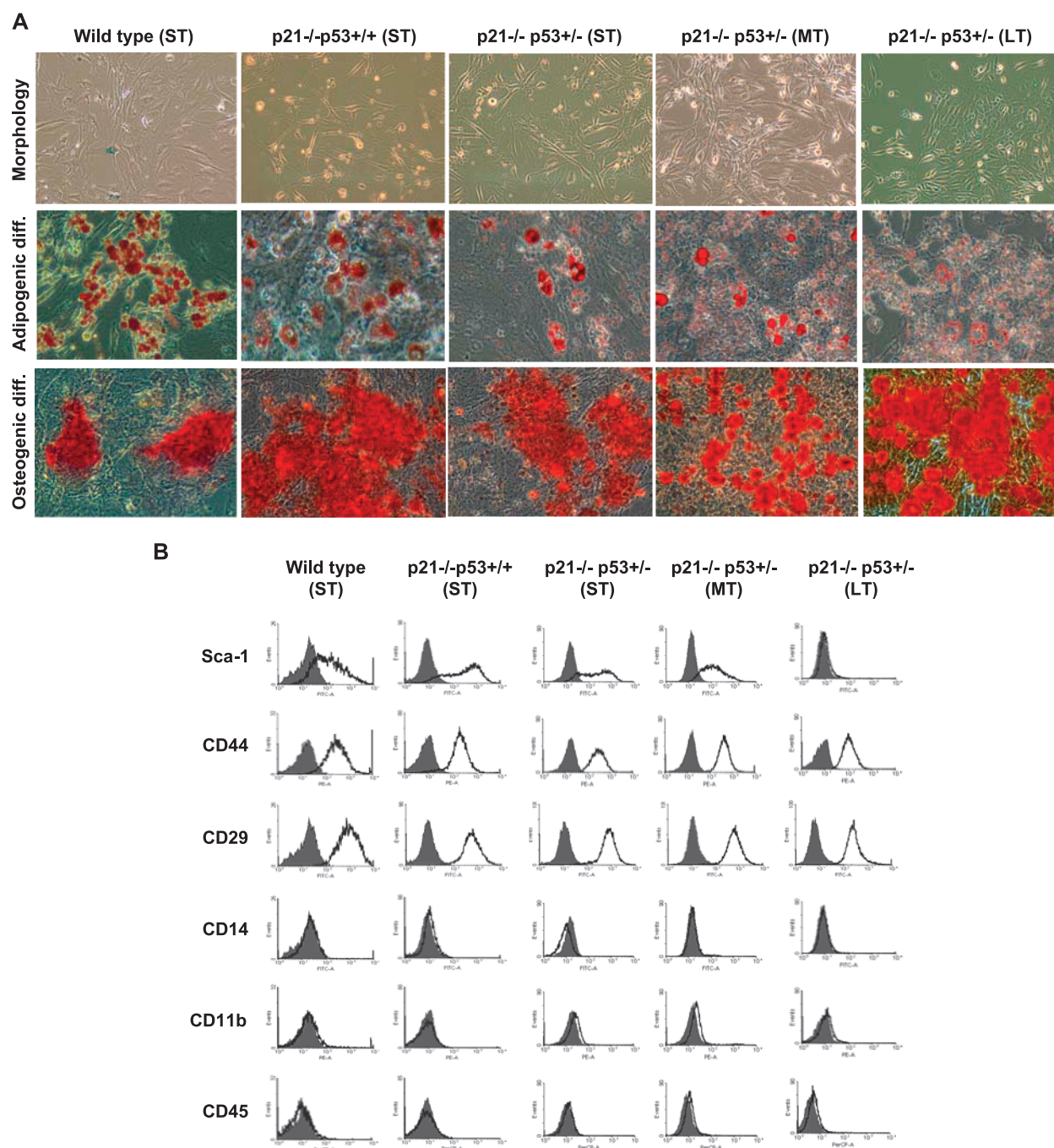


Figure 1. MSCs characterization. (A) Morphology, Oil Red O staining (adipogenic differentiation), and Alizarin Red staining (osteogenic differentiation) of the indicated MSCs. Original magnification, $\times 20$. (B) Fluorescence-activated cell sorting analysis of MSC surface markers. Filled line, control isotype; empty line, cells incubated with the indicated antibody.

Karyotypic analysis showed moderate levels of chromosomal instability in *wild-type* and *p21^{-/-}p53^{+/+}* MSCs as expected for primary cultures of mouse cells. Nevertheless, relevant differences in the level of instability have been found. Thus, approximately 50% to 60% of metaphases from *wild-type* (ST) and *p21^{-/-}p53^{+/+}* (ST) MSCs cultures showed normal karyotypes. The rest of the metaphases gained chromosomes, showing most of them a karyotype with 41 to 70 chromosomes (Figure W1, A and B). Conversely, cultures from *p21^{-/-}p53^{+/-}* (ST) showed a higher level of chromosomal instability, because virtually, the whole population had gained

extra chromosomes, with 80% of them displaying karyotypes of more than 70 chromosomes. After LT culture, these cells showed a kind of adaptation to *in vitro* culture conditions and lost some of the previously gained chromosomes (Figure W1, A and B). Cell cycle analysis of these cells confirm that *p21^{-/-}p53^{+/-}* (ST) had almost double DNA content than *wild-type* or *p21^{-/-}p53^{+/+}* cells and that *p21^{-/-}p53^{+/-}* (LT) presented an intermediate amount of DNA content (Figure W1C). Cell cycle profiles also revealed a higher proportion of cells in S-phase in *p21^{-/-}p53^{+/-}* (LT; 23.20%) compared with *p21^{-/-}p53^{+/-}* (ST; 17.89%) cells and especially to

wild-type (9.09%) and $p21^{-/-}p53^{+/+}$ (9.05%) cells according to their growth rates.

Loss of p53 and p16 Expression in $p21^{-/-}p53^{+/+}$ MSCs After Long-term Cell Culture

To better understand the observed transformation of $p21^{-/-}p53^{+/+}$ after LT *in vitro* culture, we analyzed the expression of relevant cell cycle regulators in control conditions or after a 24-hour treatment with the topoisomerase I inhibitor CPT, which induces DNA damage in the form of replication fork stress, as a control for the activation of some of these proteins (Figure 3A). As expected, expression of p21 was completely absent in all of the $p21^{-/-}$ MSCs, whereas it was highly expressed and further upregulated after CPT treatment in *wild-type* cells. Conversely, expression of p53 was similar in *wild-type* and $p21^{-/-}p53^{+/+}$ (ST) cells and was slightly lower in $p21^{-/-}p53^{+/+}$ cells. A strong activation (up-regulation and phosphorylation in serine 15)

of p53 was also observed after CPT treatment of these cells. More importantly, the expression and activation of this protein were highly abrogated in $p21^{-/-}p53^{+/+}$ (MT) cells and completely disappeared in $p21^{-/-}p53^{+/+}$ (LT) MSCs.

We next analyzed the expression of the proteins codified by the INK4A/ARF locus p16 and p19 whose altered expressions have been reported in other models of transformed MSCs [23,35]. The expression pattern of p16 was similar to that observed for p53, showing a high expression level in *wild type*, $p21^{-/-}p53^{+/+}$, and $p21^{-/-}p53^{+/+}$ (ST) cells, a great reduction of their levels in $p21^{-/-}p53^{+/+}$ (MT), and complete absence of expression in $p21^{-/-}p53^{+/+}$ (LT) MSCs. Opposite to p16, p19 was poorly expressed in *wild-type* and $p21^{-/-}p53^{+/+}$ cells but highly expressed in $p21^{-/-}p53^{+/+}$ independently of their time in culture (Figure 3A).

Overexpression of c-myc is a common event associated with tumoral transformation of MSCs [22,23]. Compared with *wild-type*

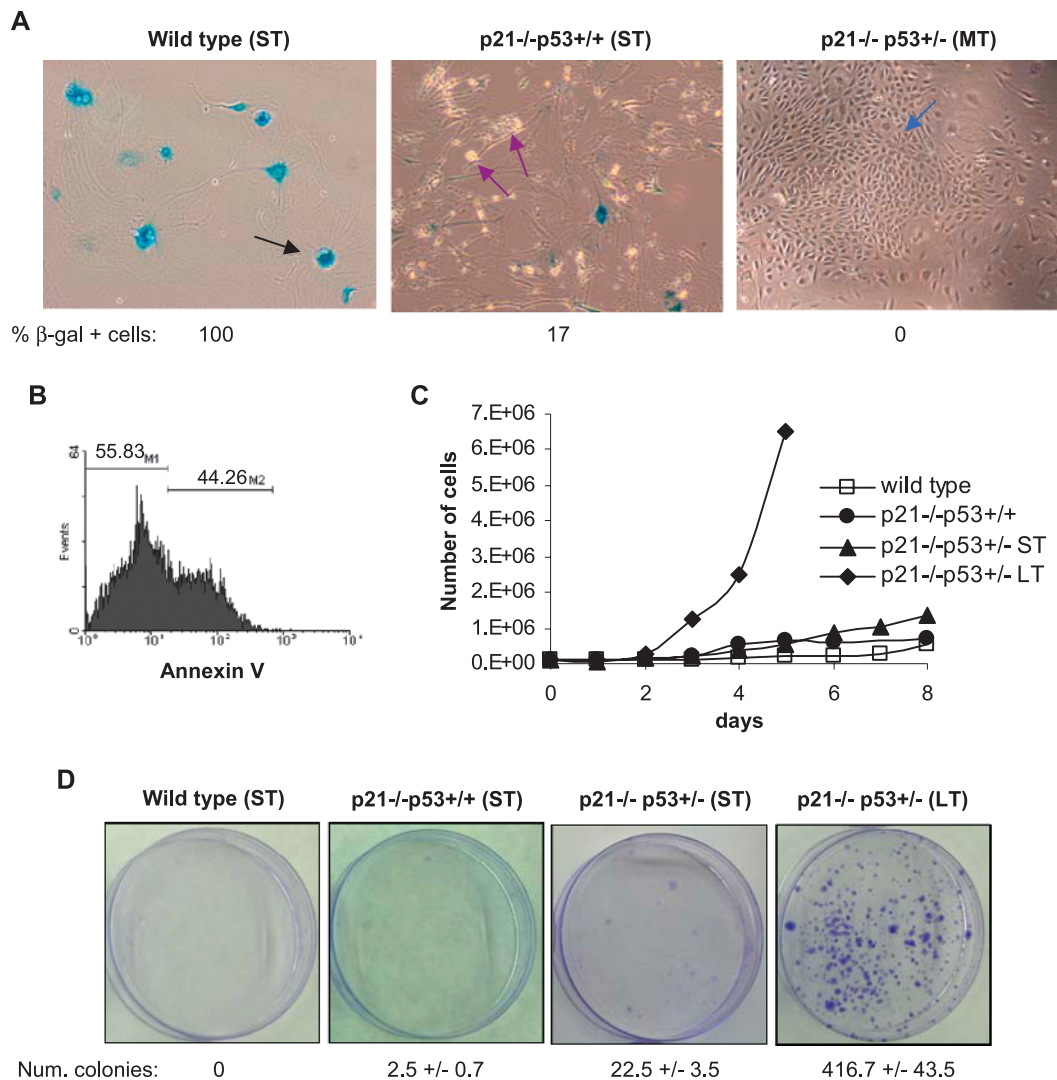


Figure 2. $p21^{-/-}p53^{+/+}$ MSCs were transformed after extensive *in vitro* culture. (A) Representative images of senescence-associated β -galactosidase (SA- β -gal) assays of *wild-type* (passage 12), $p21^{-/-}p53^{+/+}$ (passage 11), and $p21^{-/-}p53^{+/+}$ (passage 20) MSCs. SA- β -gal senescent-positive cells (black arrows), apoptotic cells (red arrows), and the outgrowth of a transformed population (blue arrow) are indicated. Original magnification, $\times 20$. (B) Annexin V binding assay of a culture of $p21^{-/-}p53^{+/+}$ (ST) cells. (C) Growth curves of the indicated MSCs. (D) Representative plates of colony formation assays showing the gain of clonogenic capacity of $p21^{-/-}p53^{+/+}$ (LT) MSCs.

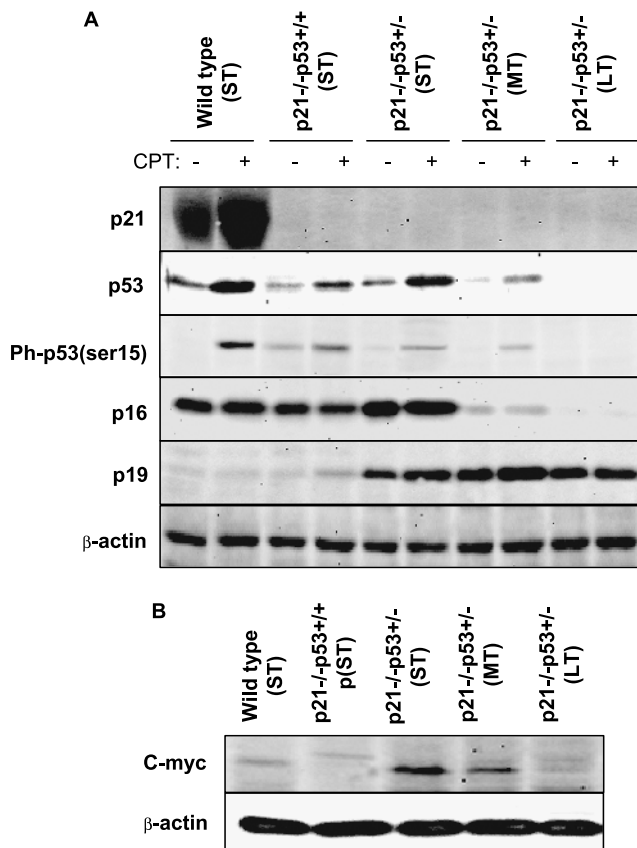


Figure 3. p53 and p16 are gradually lost after *in vitro* culture of $p21^{-/-}p53^{+/-}$ MSCs. Levels of p21, total p53, phospho-p53 (ser 15), p16, p19 (A) and c-myc (B) in the indicated MSCs treated or not with 0.5 μ M CPT for 24 hours. β -Actin levels are presented as a loading control.

cells, the expression of this oncogenic protein was virtually undetectable in $p21^{-/-}p53^{+/+}$ (ST) cells but upregulated in $p21^{-/-}p53^{+/-}$ (ST) and, in a lower degree, in $p21^{-/-}p53^{+/-}$ (MT) cells (Figure 3B). Intriguingly, c-myc levels decrease after LT culture of $p21^{-/-}p53^{+/-}$ MSCs to the levels of *wild-type* cells. This pattern of expression agrees with previously published data, which suggest a role for c-myc in senescence bypass during spontaneous tumoral transformation of human MSCs [23,28].

Lack of Serum Deprivation Induced Senescence in $p21^{-/-}p53^{+/-}$ (LT) Cells

The induction of replicative or DNA damage-induced senescence constitutes one of the most important antitumoral barriers. In mammalian cells, senescence is dependent on functional p53/p21 and/or p16 pathways [36], which are both compromised in $p21^{-/-}p53^{+/-}$ (LT) MSCs. To test the ability of *wild-type*, $p21^{-/-}p53^{+/+}$ (ST) and $p21^{-/-}p53^{+/-}$ (LT) MSCs to senesce, the cells were deprived of serum for up to 6 days before being stained for SA- β -gal (Figure 4, A and B). Control cultures of *wild-type* and $p21^{-/-}p53^{+/+}$ (ST) showed a basal level of senescence (approximately 20%). Serum deprivation of these cells showed a similar time-dependent increase in the percentage of senescent cells, reaching a maximum of 80% after 6 days. Conversely, $p21^{-/-}p53^{+/-}$ (LT) cells did not stain at all for SA- β -gal even after 6 days of being deprived of serum. However, during the experiment, these cells became smaller, rounded, and highly re-

fringent, resembling apoptotic cells (Figure 4A). Annexin V binding experiments were done to confirm this apoptotic effect (Figure 4C). *Wild-type* cells showed only a modest apoptotic induction of 20% after 6 days of serum deprivation. Meanwhile, this apoptotic effect increased up to 40% in $p21^{-/-}p53^{+/-}$ (ST) MSCs and virtually affected the whole population in $p21^{-/-}p53^{+/-}$ (LT) MSCs after the same period. These results stress the relevance of p53, p21, and p16 in the induction of senescence and suggest an important role of this mechanism in the protection against tumoral transformation of MSCs. Nevertheless, these results also suggest that agents that induce senescence could be efficient apoptotic inducers in transformed MSCs knocked down for p53/p21 and p16 pathways.

In Vivo Tumor Formation Potential of $p21^{-/-}p53^{+/-}$ MSCs

To test the ability of $p21^{-/-}p53^{+/-}$ MSCs to form tumors *in vivo*, we introduced cells of the different studied genotypes into immunodeficient mice through subcutaneous injection. One hundred fifty days after the inoculation of *wild-type*, $p21^{-/-}p53^{+/+}$, or $p21^{-/-}p53^{+/-}$ (ST) MSCs, no signs of illness or tumor formation were observed in any mice (Table 1). In contrast, inoculation of $p21^{-/-}p53^{+/-}$ (MT) or $p21^{-/-}p53^{+/-}$ (LT) cells originated tumors in all injected mice (Figure 5). Eventually, tumors developed ulcers in the skin when the diameter reached approximately 7 to 10 mm, and the mice in these groups were killed. $p21^{-/-}p53^{+/-}$ (MT) and $p21^{-/-}p53^{+/-}$ (LT) MSCs reached this point 105 and 74 days after inoculation, respectively, evidencing the more aggressive phenotype of $p21^{-/-}p53^{+/-}$ (LT), which completely lacks p53 and p16. Anatomopathological analysis classified tumors as fibrosarcomas, showing most cells an elongated shape, anisocytosis, anisokaryosis, and an elevated mitotic index (Figure 5). Tumors obtained from $p21^{-/-}p53^{+/-}$ (MT) showed areas of adipose tissue differentiation, whereas tumors from $p21^{-/-}p53^{+/-}$ (LT) MSCs displayed not only adipose but also osteocytic differentiation as well as signs of neural differentiation, as indicated by β -tubulin III staining of cells residing inside nerve-like structures (Figure 5). Moreover, small nodules of metastasis were found in lungs from some mice (Figure 5).

In addition, we have also tested the ability of $p21^{-/-}p53^{+/+}$ and $p21^{-/-}p53^{+/-}$ (LT) MSCs to form tumors *in vivo* in an environment characteristic of MSCs such as bone marrow. Thus, MSCs were injected into the femurs of immunodeficient mice (Table 1). Again, no tumors were observed from $p21^{-/-}p53^{+/+}$ MSCs. Conversely, all the mice injected with $p21^{-/-}p53^{+/-}$ (LT) MSCs developed fibrosarcomas with some level of fat differentiation, present both inside the bone marrow and infiltrated between the muscles surrounding the bone (Figure 5). Altogether, these results confirm that p21 knockdown *per se* is not enough to transform MSCs, but simultaneous and gradual loss of p53 and p16 expression cooperate to induce an increasingly aggressive tumorigenic phenotype.

Characterization of Cells Derived from $p21^{-/-}p53^{+/-}$ MSC-Induced Tumors

We next extracted and cultured cells from tumors derived from $p21^{-/-}p53^{+/-}$ (MT) (Tp21p53/MT) and from $p21^{-/-}p53^{+/-}$ (LT) cells (Tp21p53/LT). Cells from both tumors showed similar growth properties compared with their parental MSCs, including morphology (Figure 6A), absence of contact inhibition, elevated mitotic index, and clonogenic capacity (data not shown). Tp21p53/MT and LT cells were negative for CD45, CD14 and CD11b, positive for CD44 and CD29 and weakly positive for Sca-1 (Figure 6B),

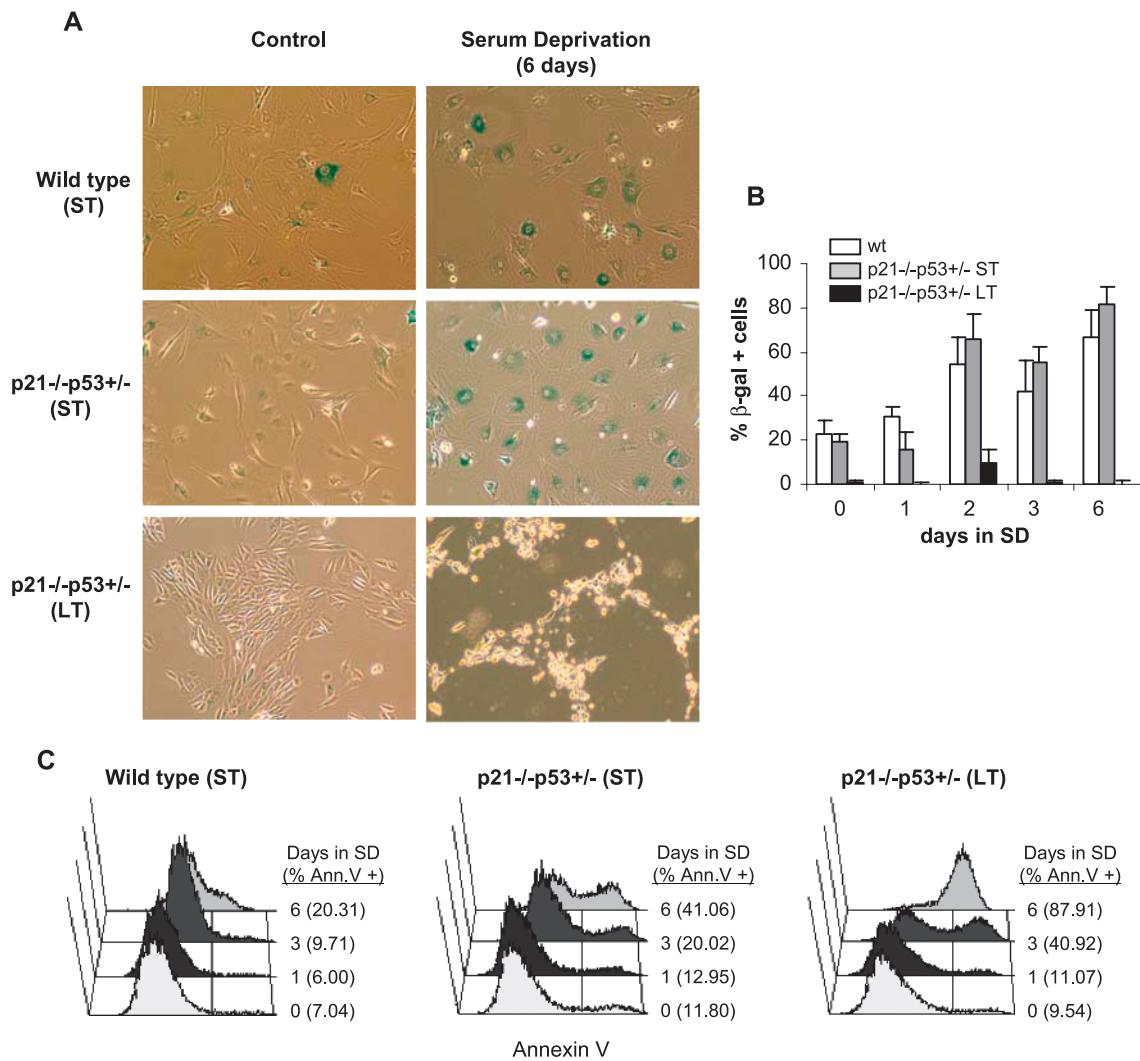


Figure 4. Senescence induction after serum deprivation of $p21^{-/-}p53^{+/-}$ MSCs. The indicated MSCs were deprived of serum for the indicated days and analyzed for senescence-associated β -galactosidase (SA- β -gal) activity (A, representative images; original magnification, $\times 20$; B, mean and SD of three independent experiments) or for the Annexin V binding (C, percentage of Annexin V-positive apoptotic cells is indicated).

similar to the parental MSCs. These cells showed a strong ability for osteogenic differentiation together with a weak differentiation to adipocytes (Figure 6A), similar to that reported for $p53^{-/-}$ MSCs [37]. Indeed, both Tp21p53/MT and Tp21p53/LT cells did not express p21 or p53 proteins (Figure 6C). Like the parental MSCs, Tp21p53/MT showed a reduced expression of p16, which was completely absent in Tp21p53/LT cells, whereas the p19 levels were highly upregulated in both type of cells compared with wild-type

MSCs. Likewise, c-myc levels were similar in wild-type and both tumor-derived cells, following the pattern of expression of their parental MSCs (Figure 6D).

Tumor-derived cells also showed a great increase in the number of chromosomes, presenting a medium of 63 chromosomes in Tp21p53/MT and 75 in Tp21p53/LT cells (Figure W2A). The differences in DNA content were also confirmed by cell cycle analysis (Figure W2B). Percentage of cells in the S phase in tumor-derived

Table 1. *In Vivo* Tumor Formation Ability of $p21^{-/-}$ MSCs.

	Subcutaneous Injection			Intrafemoral Injection	
	Tumors/Mice	Days to Tumor Development*	Histologic Analysis	Tumors/Mice	Histologic Analysis
<i>wild-type</i>	0/5	NT [†]	Normal	—	—
$p21^{-/-}p53^{+/+}$	0/5	NT [†]	Normal	0/4	Normal
$p21^{-/-}p53^{+/-}$ ST	0/5	NT [†]	Normal	—	—
$p21^{-/-}p53^{+/-}$ MT	5/5	105	Fibrosarcoma + fat	—	—
$p21^{-/-}p53^{+/-}$ LT	5/5	74	Fibrosarcoma + fat + bone + nerve	4/4	Fibrosarcoma + fat

*Average number of days needed to observe tumor ulceration and an approximate tumor diameter of 8 mm. Mice carrying tumors were killed at this point.

[†]NT, no tumors were detected. Mice were killed 150 days after injection.

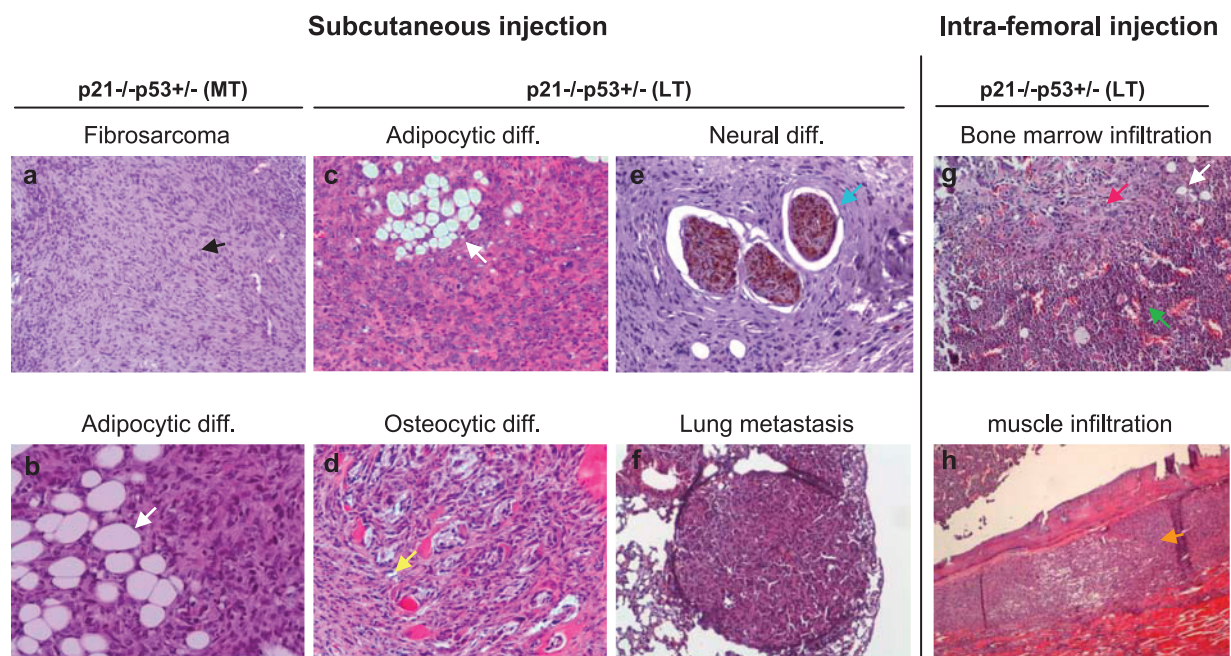


Figure 5. *In vivo* tumor formation ability of transformed $p21^{-/-}p53^{+/-}$ MSCs. Hematoxylin and eosin staining (and β -tubulin III immunohistochemistry for e) of tumors obtained after subcutaneous or intrafemoral injection of $p21^{-/-}p53^{+/-}$ (MT) and $p21^{-/-}p53^{+/-}$ (LT) as indicated. Tumors generated after subcutaneous injection were mostly composed of elongated cells typical of fibrosarcomas (a, black arrow) showing anisocytosis, anisokaryosis and an elevated mitotic index. These tumors also showed areas of adipose tissue differentiation (b, c, white arrows), osteogenic differentiation (d, yellow arrow) and nerve-like structures showing positive staining for β -tubulin III (e, blue arrow). Lungs infiltrated with $p21^{-/-}p53^{+/-}$ transformed MSCs were observed in some mice (f). Tumors generated after intrafemoral injection of $p21^{-/-}p53^{+/-}$ (LT) MSCs showed the same fibrosarcoma morphology and were present both inside the bone marrow (g, see red arrow for tumor cells, white arrow for adipose differentiation, and green arrow for bone marrow) and infiltrated between the muscle surrounding the bone (h, orange arrow). Original magnifications: all (except in b and f, $\times 10$), $\times 4$.

cells (22.07% for Tp21p53/MT cells and 23.81% for Tp21p53/LT cells) was again similar to that observed in their parental MSCs. In summary, the cells recovered from tumors showed a phenotype and biological behavior similar to that observed in the parental transformed MSCs, $p21^{-/-}p53^{+/-}$ (MT) and $p21^{-/-}p53^{+/-}$ (LT).

Discussion

$p21$ plays important roles in regulating key antitumoral barriers such as cell cycle control, senescence, and apoptosis, and its deficiency predisposes mice to spontaneous and induced tumorigenesis. Most of these spontaneous tumors observed in $p21$ knockout mice were sarcomas [8], and $p21$ deficiency also increased the percentage of sarcomas in $p53$ -deficient mice [9]. These data suggest a potential link between $p21$ deficiency and sarcomagenesis. In addition, human and mouse MSCs transformed after *in vitro* culture generated sarcomas *in vivo* [21–24], and human MSCs have been proposed as cancer stem cells for certain sarcomas [16–20]. Thus, we wanted to test if $p21$ -deficient MSCs could be transformed *in vitro* and form sarcomas *in vivo*.

Our study suggests that $p21$ deficiency is not enough for MSC immortalization, even losing one allele of $p53$. However, serial cultivation of $p21^{-/-}p53^{+/-}$ mMSCs was accompanied of a total loss of heterozygosity in $p53$ function. As a result, long-term cultured $p21^{-/-}p53^{+/-}$ mMSCs became immortalized and were able to induce tumor formation into immunodeficient mice, according to the two-hit model of tumorigenesis (see Figure W3 for a summary of the transforming events observed in the MSCs cultures). Altogether,

we conclude that the deficiency of $p21$ and $p53$ would generate sarcomas from MSCs.

According to our data, it has been reported that the loss of $p21$ accelerated tumor onset in mice deficient for $p53$ -induced apoptotic function, and these tumors showed an increased CIN [38]. We found a similar increase in CIN in $p21^{-/-}p53^{+/-}$ MSCs even after a short number of passages when $p53$ protein is still expressed and can be phosphorylated after DNA damage, suggesting that $p53$ is haploinsufficient to maintain chromosomal stability in a $p21^{-/-}$ background.

Loss of heterozygosity has previously been reported after *in vitro* culture of $p21$, $p53$, Rb , or $p16$ heterozygous human fibroblasts [39]. In this case, cells that lost heterozygosity for $p21$, $p53$, and Rb but not for $p16$ were able to bypass senescence, although the extended life span of these cells eventually terminated in a crisis state. Likewise, fibroblast from patients with Li-Fraumeni syndrome ($p53^{+/-}$) spontaneously lost the wild-type $p53$ allele and gained extended life span [40]. Moreover, spontaneous immortalization of murine fibroblasts is frequently associated with a mutation of $p53$ [41], and wild-type and $p21^{-/-}$ MEF cultures acquire alterations in $p53$ [42]. In MSCs, genetic changes, in particular, $p53$ mutations, occur after long-term *in vitro* proliferation [21]. In our model, $p21^{-/-}p53^{+/-}$ mMSCs, which completely lost $p53$ expression, became not only immortalized but also transformed, suggesting an important role for $p21$ in the prevention of tumorigenesis in MSCs.

Loss of $p21$ also permits carcinogenesis in chronically damaged epithelial cells despite having lost the $p21$ antiapoptotic functions [43]. We have also noticed a higher apoptosis rate in $p21^{-/-}$ MSC

cultures, and similar observations have been reported in other cell types. Thus, *p21*^{-/-} mice show a defect in the induction of p53-mediated G₁/S arrest in response to γ -radiation [7] but maintain an intact apoptotic response [29]. In addition, irradiation-induced thymic lymphomas in *p21*-null mice show a significantly higher level of apoptosis compared with that in *wild-type* mice [8]. Moreover, lymphocytes in the spleen of *p21*-deficient mice display a higher level of constitutive apoptosis compared with *wild-type* mice [44].

Other alterations detected during the *in vitro* culture of *p21*^{-/-}*p53*^{+/-} MSCs included the loss of p16 expression accompanied by a high

up-regulation of the related tumor-suppressor protein p19 and a transient up-regulation of *c-myc*. p16 and p19 are encoded by overlapping reading frames in the same gene (*INK4/ARF*), so p16 silencing is not due to the loss of this locus. In this regard, it has been reported that p16 expression is closely associated with senescence of human MSCs and could be silenced by DNA methylation during *in vitro* expansion of these cells [45]. Repression of p16 expression has also been reported in a case of spontaneous transformation of human MSCs [23,28]. Another study shows that the loss of p16 with retention of p19 is enough to predispose mice to tumorigenesis [46].

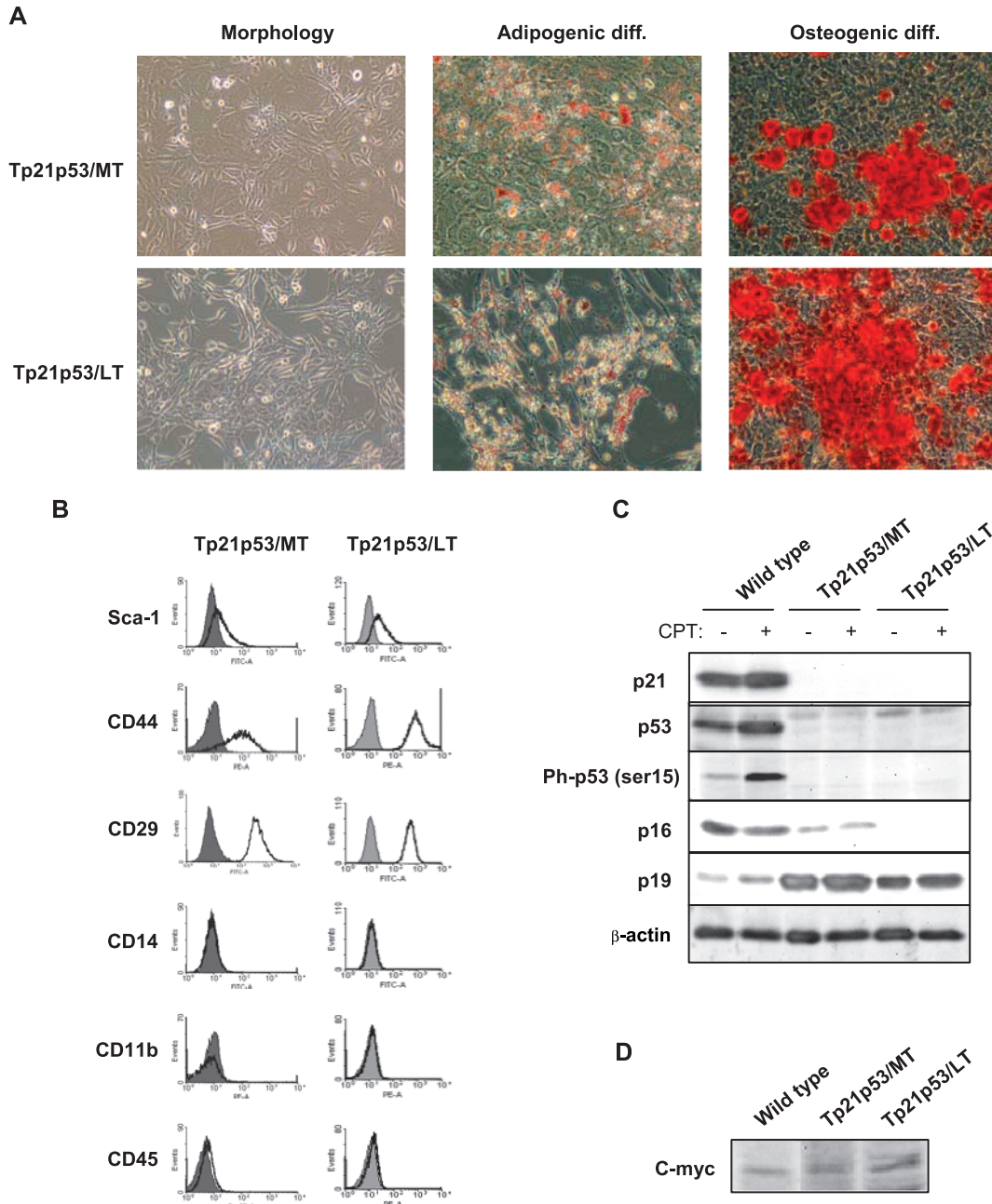


Figure 6. Characterization of cell lines derived from *p21*^{-/-}*p53*^{+/-} MSCs-induced tumors. (A) Morphology, Oil Red O staining (adipogenic differentiation), and Alizarin Red staining (osteogenic differentiation) of the indicated tumor-derived cells. Original magnification, $\times 20$. (B) Fluorescence-activated cell sorting analysis of MSCs surface markers. (C) Levels of p21, total p53, phospho-p53 (ser 15), p16, and p19 in *wild-type* MSCs or tumor-derived cell lines treated or not with 0.5 μ M CPT for 24 hours. β -Actin levels are presented as a loading control. (D) c-myc levels in the indicated cells. Loading controls are the same as in (C).

p19 regulates a route for p53 stabilization in response to aberrant growth or oncogenic stresses [47]. We hypothesized that the high levels of p19 observed could be due to an insufficient activation of p53 in $p53^{+/-}$ and $p53^{-/-}$ MSCs in response to the high level of CIN and/or the c-myc up-regulation observed after *in vitro* culture of these cells.

Activation of c-myc has been demonstrated as a very relevant event in the transformation process of human MSCs [48], being commonly upregulated in cases of transformation of human and mMSCs [22,23]. The transient up-regulation of c-myc in MSCs has been associated with the bypass of cellular senescence [28].

In mammalian cells, senescence is initiated by one of these two signaling pathways: p53/p21 and p16/Rb [36]. In human fibroblasts, it has been shown that the up-regulation of p21 is the primary response-inducing cellular senescence, whereas the up-regulation of p16 occurs weeks after the induction of cell cycle arrest [49]. In this regard, the inactivation of p21 and INK4 pathways in a mouse model strongly cooperates in suppressing cellular senescence [50]. Interestingly, this double mutant displays an increased incidence of sarcomas compared with the single mutants. In our model, the loss of p21, p53, and p16 suppresses not only replicative but also serum deprivation-induced senescence. Intriguingly, $p21^{-/-}p53^{+/-}$ (LT) cells that do not senesce after 6 days of serum deprivation undergo a p53-independent apoptotic cell death, suggesting that agents that induce senescence could be efficient apoptotic inducers in transformed MSCs deficient for p53/p21 and p16 pathways.

In summary, transformation of MSCs seems to be highly dependent on alterations in the p21/p53 pathway. Our data indicate that p21-deficiency itself is not sufficient to allow MSCs immortalization. However, when the p21 deficiency is coupled to p53 deficiency, the MSCs bypass senescence *in vitro* and generate tumors that resemble typical mesenchymal sarcomas *in vivo*. Our study suggests the hypothesis that MSCs might require few genetic alterations to undergo transformation and may act as the cellular origin for sarcomas.

References

- [1] el-Deiry WS, Tokino T, Velculescu VE, Levy DB, Parsons R, Trent JM, Lin D, Mercer WE, Kinzler KW, and Vogelstein B (1993). WAF1, a potential mediator of p53 tumor suppression. *Cell* **75**, 817–825.
- [2] Xiong Y, Hannon GJ, Zhang H, Casso D, Kobayashi R, and Beach D (1993). p21 is a universal inhibitor of cyclin kinases. *Nature* **366**, 701–704.
- [3] Brown JP, Wei W, and Sedivy JM (1997). Bypass of senescence after disruption of $p21^{CIP1/WAF1}$ gene in normal diploid human fibroblasts. *Science* **277**, 831–834.
- [4] Han Z, Wei W, Dunaway S, Darnowski JW, Calabresi P, Sedivy J, Hendrickson EA, Balan KV, Pantazis P, and Wyche JH (2002). Role of p21 in apoptosis and senescence of human colon cancer cells treated with camptothecin. *J Biol Chem* **277**, 17154–17160.
- [5] Janicke RU, Sohn D, Essmann F, and Schulze-Osthoff K (2007). The multiple battles fought by anti-apoptotic p21. *Cell Cycle* **6**, 407–413.
- [6] Rodriguez R and Meuth M (2006). Chk1 and p21 cooperate to prevent apoptosis during DNA replication fork stress. *Mol Biol Cell* **17**, 402–412.
- [7] Deng C, Zhang P, Harper JW, Elledge SJ, and Leder P (1995). Mice lacking $p21^{CIP1/WAF1}$ undergo normal development, but are defective in G₁ checkpoint control. *Cell* **82**, 675–684.
- [8] Martin-Caballero J, Flores JM, Garcia-Palencia P, and Serrano M (2001). Tumor susceptibility of p21(Waf1/Cip1)-deficient mice. *Cancer Res* **61**, 6234–6238.
- [9] De la Cueva E, Garcia-Cao I, Herranz M, Lopez P, Garcia-Palencia P, Flores JM, Serrano M, Fernandez-Piqueras J, and Martin-Caballero J (2006). Tumorigenic activity of p21^{Waf1/Cip1} in thymic lymphoma. *Oncogene* **25**, 4128–4132.
- [10] Wei W and Sedivy JM (1999). Differentiation between senescence (M1) and crisis (M2) in human fibroblast cultures. *Exp Cell Res* **253**, 519–522.
- [11] Cheng T, Rodrigues N, Shen H, Yang Y, Dombkowski D, Sykes M, and Scadden DT (2000). Hematopoietic stem cell quiescence maintained by p21^{Cip1/Waf1}. *Science* **287**, 1804–1808.
- [12] Kippin TE, Martens DJ, and van der Kooy D (2005). p21 loss compromises the relative quiescence of forebrain stem cell proliferation leading to exhaustion of their proliferation capacity. *Genes Dev* **19**, 756–767.
- [13] Bruhl T, Heeschen C, Aicher A, Jadidi AS, Haendeler J, Hoffmann J, Schneider MD, Zeicher AM, Dimmeler S, and Rossig L (2004). p21^{Cip1} levels differentially regulate turnover of mature endothelial cells, endothelial progenitor cells, and *in vivo* neovascularization. *Circ Res* **94**, 686–692.
- [14] van den Bos C, Silverstetter S, Murphy M, and Connolly T (1998). p21(cip1) rescues human mesenchymal stem cells from apoptosis induced by low-density culture. *Cell Tissue Res* **293**, 463–470.
- [15] Zhou S, Greenberger JS, Epperly MW, Goff JP, Adler C, Leboff MS, and Glowacki J (2008). Age-related intrinsic changes in human bone-marrow-derived mesenchymal stem cells and their differentiation to osteoblasts. *Aging Cell* **7**, 335–343.
- [16] Li H, Fan X, Kovi RC, Jo Y, Moquin B, Konz R, Stoicov C, Kurt-Jones E, Grossman SR, Lyle S, et al. (2007). Spontaneous expression of embryonic factors and p53 point mutations in aged mesenchymal stem cells: a model of age-related tumorigenesis in mice. *Cancer Res* **67**, 10889–10898.
- [17] Matushansky I, Hernando E, Socci ND, Mills JE, Matos TA, Edgar MA, Singer S, Maki RG, and Cordon-Cardo C (2007). Derivation of sarcomas from mesenchymal stem cells via inactivation of the Wnt pathway. *J Clin Invest* **117**, 3248–3257.
- [18] Riggi N, Cironi L, Provero P, Suva ML, Kaloulis K, Garcia-Echeverria C, Hoffmann F, Trumpp A, and Stamenkovic I (2005). Development of Ewing's sarcoma from primary bone marrow-derived mesenchymal progenitor cells. *Cancer Res* **65**, 11459–11468.
- [19] Riggi N, Cironi L, Provero P, Suva ML, Stehle JC, Baumer K, Guillou L, and Stamenkovic I (2006). Expression of the FUS-CHOP fusion protein in primary mesenchymal progenitor cells gives rise to a model of myxoid liposarcoma. *Cancer Res* **66**, 7016–7023.
- [20] Riggi N, Suva ML, Suva D, Cironi L, Provero P, Tercier S, Joseph JM, Stehle JC, Baumer K, Kindler V, et al. (2008). EWS-FLI-1 expression triggers an Ewing's sarcoma initiation program in primary human mesenchymal stem cells. *Cancer Res* **68**, 2176–2185.
- [21] Tirode F, Laud-Duval K, Prieur A, Delorme B, Charbord P, and Delattre O (2007). Mesenchymal stem cell features of Ewing tumors. *Cancer Cell* **11**, 421–429.
- [22] Miura M, Miura Y, Padilla-Nash HM, Molinolo AA, Fu B, Patel V, Seo BM, Sonoyama W, Zheng JJ, Baker CC, et al. (2006). Accumulated chromosomal instability in murine bone marrow mesenchymal stem cells leads to malignant transformation. *Stem Cells* **24**, 1095–1103.
- [23] Rubio D, Garcia-Castro J, Martin MC, de la Fuente R, Cigudosa JC, Lloyd AC, and Bernad A (2005). Spontaneous human adult stem cell transformation. *Cancer Res* **65**, 3035–3039.
- [24] Tolar J, Nauta AJ, Osborn MJ, Panoskaltsis Mortari A, McElmurry RT, Bell S, Xia L, Zhou N, Riddle M, Schroeder TM, et al. (2007). Sarcoma derived from cultured mesenchymal stem cells. *Stem Cells* **25**, 371–379.
- [25] Liu C, Chen Z, Chen Z, Zhang T, and Lu Y (2006). Multiple tumor types may originate from bone marrow-derived cells. *Neoplasia* **8**, 716–724.
- [26] Rubio D, Garcia S, De la Cueva T, Paz MF, Lloyd AC, Bernad A, and Garcia-Castro J (2008). Human mesenchymal stem cell transformation is associated with a mesenchymal-epithelial transition. *Exp Cell Res* **314**, 691–698.
- [27] Mueller LP, Luetzkendorf J, Mueller T, Reichelt K, Simon H, and Schmol HJ (2006). Presence of mesenchymal stem cells in human bone marrow after exposure to chemotherapy: evidence of resistance to apoptosis induction. *Stem Cells* **24**, 2753–2765.
- [28] Rubio D, Garcia S, Paz MF, De la Cueva T, Lopez-Fernandez LA, Lloyd AC, Garcia-Castro J, and Bernad A (2008). Molecular characterization of spontaneous mesenchymal stem cell transformation. *PLoS ONE* **3**, e1398.
- [29] Brugarolas J, Chandrasekaran C, Gordon JI, Beach D, Jacks T, and Hannon GJ (1995). Radiation-induced cell cycle arrest compromised by p21 deficiency. *Nature* **377**, 552–557.
- [30] Ernst H, Carlton WW, Courtney C, Rinke M, Greaves P, Isaacs KR, Krinke G, Konishi Y, Mesfin GM, and Sandusky G (2001). Soft tissue and skeletal muscle. In U Mohr (Ed.). *International Classification of Rodent Tumors. The Mouse*. Berlin, Germany: Springer-Verlag, pp. 361–388.
- [31] Rodriguez R, Gagou ME, and Meuth M (2008). Apoptosis induced by replication inhibitors in Chk1-depleted cells is dependent upon the helicase cofactor Cdc45. *Cell Death Differ* **15**, 889–898.

- [32] Nadri S, Soleimani M, Hosseni RH, Massumi M, Atashi A, and Izadpanah R (2007). An efficient method for isolation of murine bone marrow mesenchymal stem cells. *Int J Dev Biol* **51**, 723–729.
- [33] Sun S, Guo Z, Xiao X, Liu B, Liu X, Tang PH, and Mao N (2003). Isolation of mouse marrow mesenchymal progenitors by a novel and reliable method. *Stem Cells* **21**, 527–535.
- [34] Bruder SP, Jaiswal N, and Haynesworth SE (1997). Growth kinetics, self-renewal, and the osteogenic potential of purified human mesenchymal stem cells during extensive subcultivation and following cryopreservation. *J Cell Biochem* **64**, 278–294.
- [35] Shima Y, Okamoto T, Aoyama T, Yasura K, Ishibe T, Nishijo K, Shibata KR, Kohno Y, Fukiage K, Otsuka S, et al. (2007). *In vitro* transformation of mesenchymal stem cells by oncogenic H-rasVal12. *Biochem Biophys Res Commun* **353**, 60–66.
- [36] Campisi J (2005). Senescent cells, tumor suppression, and organismal aging: good citizens, bad neighbors. *Cell* **120**, 513–522.
- [37] Tataria M, Quarto N, Longaker MT, and Sylvester KG (2006). Absence of the p53 tumor suppressor gene promotes osteogenesis in mesenchymal stem cells. *J Pediatr Surg* **41**, 624–632; discussion 624–632.
- [38] Barboza JA, Liu G, Ju Z, El-Naggar AK, and Lozano G (2006). p21 delays tumor onset by preservation of chromosomal stability. *Proc Natl Acad Sci USA* **103**, 19842–19847.
- [39] Wei W, Herbig U, Wei S, Dutriaux A, and Sedivy JM (2003). Loss of retinoblastoma but not p16 function allows bypass of replicative senescence in human fibroblasts. *EMBO Rep* **4**, 1061–1066.
- [40] Rogan EM, Bryan TM, Hukku B, Maclean K, Chang AC, Moy EL, Englezou A, Warneford SG, Dalla-Pozza L, and Reddel RR (1995). Alterations in p53 and p16^{INK4} expression and telomere length during spontaneous immortalization of Li-Fraumeni syndrome fibroblasts. *Mol Cell Biol* **15**, 4745–4753.
- [41] Harvey DM and Levine AJ (1991). p53 alteration is a common event in the spontaneous immortalization of primary BALB/c murine embryo fibroblasts. *Genes Dev* **5**, 2375–2385.
- [42] Pantoja C and Serrano M (1999). Murine fibroblasts lacking p21 undergo senescence and are resistant to transformation by oncogenic Ras. *Oncogene* **18**, 4974–4982.
- [43] Willenbring H, Sharma AD, Vogel A, Lee AY, Rothfuss A, Wang Z, Finegold M, and Grompe M (2008). Loss of p21 permits carcinogenesis from chronically damaged liver and kidney epithelial cells despite unchecked apoptosis. *Cancer Cell* **14**, 59–67.
- [44] Komarova EA, Christov K, Faerman AI, and Gudkov AV (2000). Different impact of p53 and p21 on the radiation response of mouse tissues. *Oncogene* **19**, 3791–3798.
- [45] Shibata KR, Aoyama T, Shima Y, Fukiage K, Otsuka S, Furu M, Kohno Y, Ito K, Fujibayashi S, Neo M, et al. (2007). Expression of the p16^{INK4A} gene is associated closely with senescence of human mesenchymal stem cells and is potentially silenced by DNA methylation during *in vitro* expansion. *Stem Cells* **25**, 2371–2382.
- [46] Sharpless NE, Bardeesy N, Lee KH, Carrasco D, Castrillon DH, Aguirre AJ, Wu EA, Horner JW, and DePinho RA (2001). Loss of p16^{INK4a} with retention of p19^{Arf} predisposes mice to tumorigenesis. *Nature* **413**, 86–91.
- [47] Kim WY and Sharpless NE (2006). The regulation of INK4/ARF in cancer and aging. *Cell* **127**, 265–275.
- [48] Funes JM, Quintero M, Henderson S, Martinez D, Qureshi U, Westwood C, Clements MO, Bourboulia D, Pedley RB, Moncada S, et al. (2007). Transformation of human mesenchymal stem cells increases their dependency on oxidative phosphorylation for energy production. *Proc Natl Acad Sci USA* **104**, 6223–6228.
- [49] Stein GH, Drullinger LF, Soulard A, and Dulic V (1999). Differential roles for cyclin-dependent kinase inhibitors p21 and p16 in the mechanisms of senescence and differentiation in human fibroblasts. *Mol Cell Biol* **19**, 2109–2117.
- [50] Quereda V, Martinabo J, Dubus P, Carnero A, and Malumbres M (2007). Genetic cooperation between p21^{Cip1} and INK4 inhibitors in cellular senescence and tumor suppression. *Oncogene* **26**, 7665–7674.

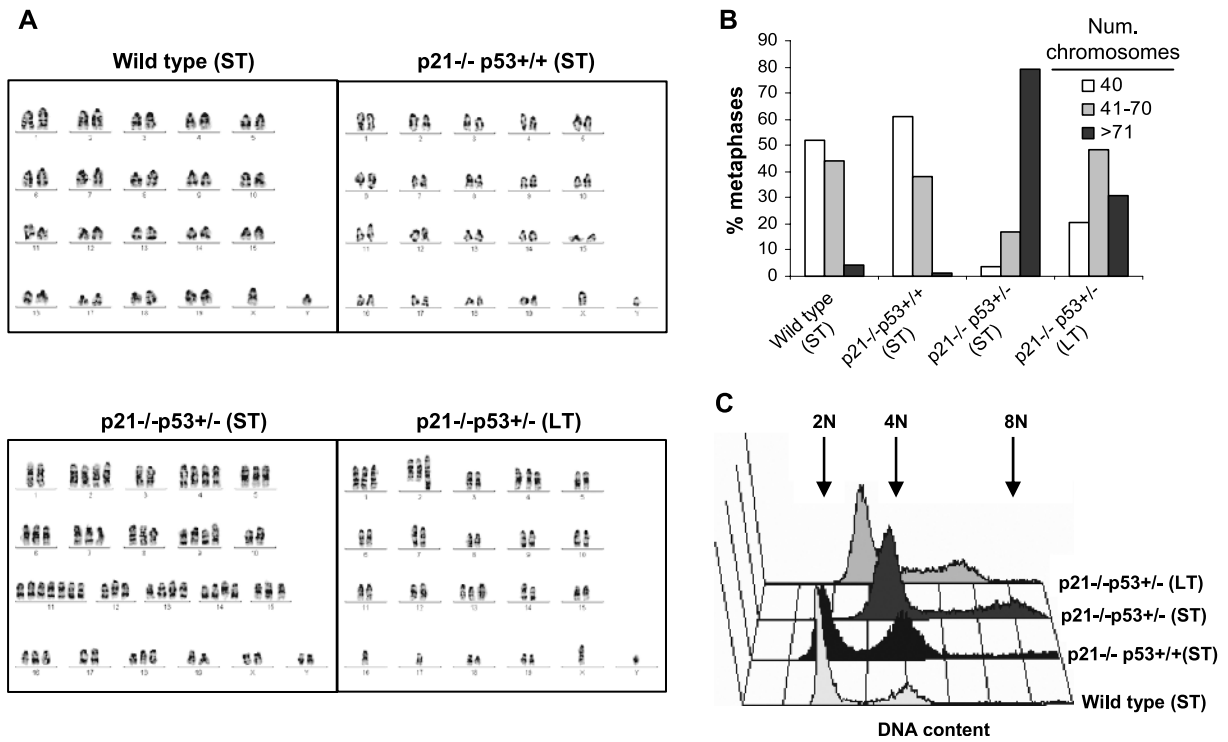


Figure W1. Genetic instability in p21^{-/-}p53^{+/-} MSCs. (A) G-banded karyotypes representative of the indicated MSCs. (B) Percentages of metaphases containing the indicated number of chromosomes. At least 50 metaphases of each MSC type were counted. (C) Cell cycle analysis of the indicated MSCs. 2N DNA content peak according to the G₁ population of wild-type MSCs and corresponding to 4N and 8N DNA content peaks are pointed.

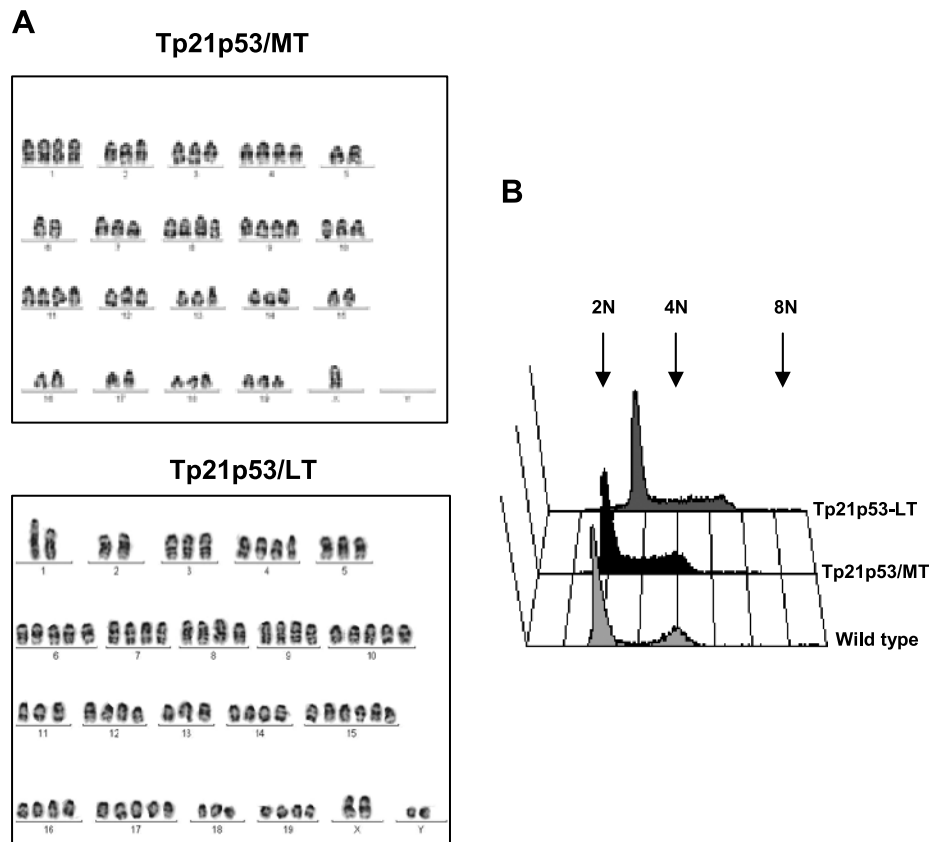


Figure W2. Genetic instability in Tp21p53 tumor cells. (A) G-banded karyotypes representative of the indicated tumor cell lines. (B) Cell cycle analysis. 2N DNA content peak according to the G_1 population of wild-type MSCs and corresponding to 4N and 8N DNA content peaks are pointed.

Summary of transforming events in p21^{-/-}p53^{+/-} MSCs cultures

		<i>in vitro</i> culture periods		
		Short term (0-15 pass.)	Medium term (16-35 pass.)	Long term (36-60 pass.)
Wild type	- senescence		No progression of cultures after senescence	
p21^{-/-}p53^{+/+}	- senescence - apoptosis		No progression of cultures after senescence/apoptosis	
p21^{-/-}p53^{+/-}	- increased chromosome instability - increased levels of c-myc	- senescence bypass - immortalization - reduction of p53 and p16 levels - <i>in vivo</i> tumorigenicity		- reduction of Sca-1 expression - complete loss of p53 and p16 - loss of serum dep. induced senescence - increased <i>in vivo</i> tumorigenicity

Figure W3. Summary of transforming events in p21^{-/-}p53^{+/-} MSCs cultures.